Comprehensive Design for a Neuro-Fuzzy Controller for a Safe Hydrogen Energy Storage

Faris N. Shaker
Electrical Power Techniques
Middle Technical University
Baghdad, Iraq
bcc0013@mtu.edu.iq

Adel A. Obed
Electrical Power Techniques
Middle Technical University
Baghdad, Iraq
adelrazan@mtu.edu.iq

Ahmed J. Abid
Electrical Power Techniques
Middle Technical University
Baghdad, Iraq
dr.ahmedjabbar@mtu.edu.iq

***Abstract*— Due to the high cost of traditional fuel and their effect on the environment, researchers save no effort in finding new alternative energy sources. Unfurchently, these alternative energy sources had high uncertainty due it is high dependence on the weather conditions. Many energy storage elements are proposed with different energy storage efficiency, cost, and limitations to solve this problem. Energy production sectors are locking in energy storage elements that can store energy to overcome the uncertainty caused by day and night conditions in a matter PV system and the long term as in wind energy or longer in a matter of hydro energy. There is no doubt that hydrogen is considered necessary alternative storage for renewable energy due to its long storage time. This paper investigates energy storage technologies that can enhance the solar energy utilization of the MPPT-connected alkaline electrolyzer, Simulink batch converter photovoltaic module, and hydrogen storage. Numerical analysis results are provided for system components while running for 24 hours under specific conditions. Combining electrolysis and the photovoltaic array is validated, and then the model parameters are adjusted based on the experimental results. This model has been applied to predict system performance. These mathematical reference models cover the transient performance and steady-state output, which are regulated by many internal factors of the Electrolyzer. The hydrogen storage produced was controlled using Neuro-Fuzzy control to increase the raise time and avoid any overshooting in the response that caused high pressure in the storage tank. The simulation results reveal that the proposed Implementation's steady-state outputs fit the system's overall response.**

Keywords*— *alkaline water electrolyzer, hydrogen storage energy, Neuro-Fuzzy.

I. INTRODUCTION

Energy storage is an essential component of smart grids and modern energy systems since it helps to improve their efficiency and resilience. Because there are so many energy storage technologies available, several essential characteristics must be examined to select the best storage options, including cost, longevity, dependability, volume, storage capacity, and environmental threats [1]. These elements must be balanced to identify the sort of storage to be added and the possible benefit from energy storage. There may be instances where adding unit storage is unnecessary to justify the cost. The three major categories are mechanical, electrochemical, and electromagnetic energy storage methods. Pumped water, compressed air energy, and flywheels are examples of mechanical storage.

On the other hand, electrochemical energy storage covers all forms of batteries and hydrogen-based energy storage, while electromagnetic energy storage includes supercapacitors and superconducting magnetic energy storage[2]. Each technology has its storage capacity, power, reaction time, and cost. The storage capacity for systems is shown in Fig.1 [3, 4]._ENREF_4

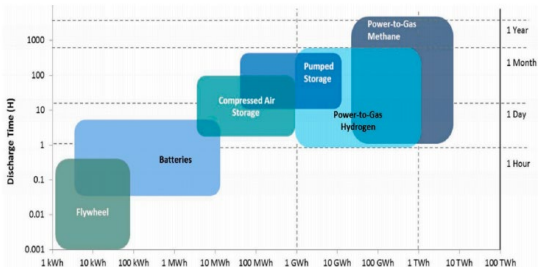

Fig. 1 Comparison of discharge time capacity of energy storage technologies

Energy storage systems offer various energy release rates (discharge rates) ranging from seconds to several hours and days. Short- and long-term energy storage systems exist, and short-range storage methods include superconducting energy storage (*SCES*), flywheel energy storage (*FES*), and magnetic superconducting energy storage (*MSCES*) (*SMEs*)[5]. Pumped hydroelectric storage (*PHES*), compressed air energy storage (*CAES*), battery energy storage (BES), and hydrogen energy storage are the different types of long-term storage systems (*HES*)[6]. Typical energy storage capacity and discharge durations for energy storage systems are shown. Fig. 2 Widespread renewable energy (solar PV and wind energy), intermittent production from problems, and increased price volatility in the electricity market[7]. Long-term storage technologies can help alleviate energy shortages, relieve system congestion, and promote distributed generation by storing power generated from renewable sources more reliably in energy storage devices[8]. When renewable energy sources are unavailable, energy storage provides a means to match supply and demand patterns, as well as an alternative energy source

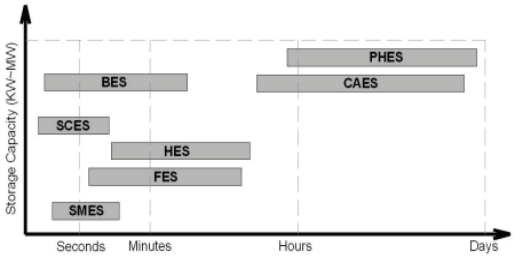

Fig. 2 Energy Discharge Time (Seconds-Hours)

Hydrogen energy storage is one of the most promising energy storage technologies[9]. Because of its environmentally friendly manufacturing, hydrogen production has several environmental consequences, depending on whether it is obtained from renewable or nonrenewable sources [10]. The electrolysis of water is the most frequently acknowledged method due to its high sustainability and low or no toxic emissions. An electrolyzer performs this chemical reaction by using two electrodes and an electrolyte. The three electrolytes are alkaline, proton exchange membrane (PEM), and solid oxide (SOE).[11].

Alkaline electrolysis is the most extensively used method for creating hydrogen from water because of its high maturity and low cost [12]. Despite technological developments, there are still several obstacles to boosting overall system efficiency and breadth of operation. A simulation is an essential tool for overcoming these difficulties and learning more about these problems. Various mathematical models of the Electrolyzer have been developed during the last three decades [13]. The models generated have earned experimental projects from the most major demonstration projects due to their correctness in replicating the functional features of genuine devices. The concept has described numerous electrolyzers in several investigations [14]. MATLAB is a simulation program with a growing user base that offers a variety of benefits for modelling numerous systems. Simscape, when combined with MATLAB/Simulink, allows users to explore mathematical models in their physical domain, making it simpler to comprehend their behaviour in the actual world and expanding the number of possible connections [15]. According to an equivalent circuit constructed for the alkaline Electrolyzer [16]. The Alkaline Electrolyzer System Model and the Simulink Simscape System Model were created from the ground up using a mix of mathematical formulas and real-world data obtained from multiple sources. Both sections are thoroughly detailed to establish whether their reactions are consistent with the desired outcome [17]. The photovoltaic system with hydrogen storage was modeled and operated in terms of energy production, and analyzes were performed with the support of experimental data for a renewable energy system consisting of photovoltaic modules, a fuel cell, electrolyzers, and hydrogen storage. The hydrogen storage produced was controlled using Neuro-Fuzzy control to increase the raise time and avoid any overshooting in the response that caused high pressure of the storage tank. This control reduces the risk of explosion and increases system stability.

II. METHODOLOGY

Construct their models using physical and chemical concepts and experimental criteria. Each physical component of the proposed system is modelled as a block and simulation complex using a conventional systems simulation tool. The models must be as generic as possible, which is accomplished by including design factors (such as the number of cells in series or parallel) and manufacturer-supplied component characteristics in each block (e.g., voltage-current curve). Simulink allows for visualizing hierarchical building models at multiple levels of abstraction. Each block may include "other blocks, other levels." The solar cell and the method for adjusting the strength of the radiation have been modelled (MPPT modelled P&O). Modeling of DC-DC energy convex devices is also an option (boost converter and buck converter). This package also includes modelling an alkaline electrolyzer and a hydrogen gas storage system with intelligent control of the storage system, as shown in Fig. 3.

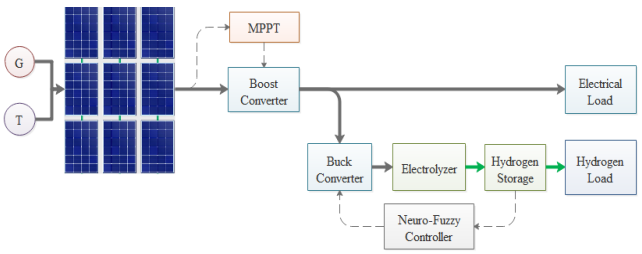

Fig. 3 Energy storage system diagram

A. PV Modelling

The most fundamental component of the *PV* conversion system is the *PV* cell, which is a simple P-N junction. The equivalent circuit for the PV cell is based on the well-known single-diode mode. There is a current source (photocurrent), a diode (D), series resistance (R_s) that shows the internal resistance to current flow, and parallel resistance (R_{sh}) that shows the leakage current. The current-voltage (I - V) parameters of the *PV* cell are as follows (1):

$$I = I_{ph} - I_s\left\{exp\left[\frac{q(V+IR_s)}{A.K.T}\right]-1\right\}-\left(\frac{V+IR_s}{R_{sh}}\right) \quad (1)$$

The photovoltaic cell's operating temperature and the quantity of solar radiation have the most significant impact on the light-generating current (I ph), which is represented as in (2):

$$I_{ph} = \left[I_{sc} + K_i(T - T_{ref})\right].\left(\frac{G}{1000}\right) \quad (2)$$

The photovoltaic saturation current (Is) changes cubically with the solar cell's temperature (T), as presented in (3).

$$I_s = I_{rs}\left(\frac{T}{T_{ref}}\right)^3 exp\left[\frac{q.E_g}{K.A}\left(\frac{1}{T_{ref}}-\frac{1}{T}\right)\right] \quad (3)$$

The following (4) approximates the reverse saturation current (I_{rs}):

$$I_{rs} = \frac{I_{sc}}{\left[exp\left(\frac{qV_{oc}}{N_{ser}A.K.T}\right)-1\right]} \quad (4)$$

The solar cell's I-V and P-V characteristics influence how much power it can generate. Consequently, PV cells must be combined to give sufficient current and voltage for practical application. The photovoltaic cell's I-V and P-V characteristics govern how much power it can generate; as a consequence, PV cells must be combined to give the appropriate current and voltage for practical use [18]. Photovoltaic cells are wired in series to get the maximum voltage and achieve the largest current in parallel. Because incident radiation intensity and temperature affect voltage and current, Isc influences the intensity of incoming radiation. The open-circuit voltage (Voc) is mostly impacted by the temperature of the solar PV array. The quantity of power and current produced by the PV group has a nonlinear relationship with solar radiation. [19].

B. Maximum Power Point Tracking

The amount of solar energy that reaches the photovoltaic array varies depending on several circumstances, including the time of day, meteorological influences like clouds, and the location's latitude[20]. As a result, MPPT techniques regulate the PV array's output voltage and current to extract the most power and enhance overall PV system efficiency during solar radiation changes. The applied technique (P & O) demonstrates how to reach the entire power point (MPP) by lowering the gradient of the power-voltage (P-V) curve to zero, as shown in Fig. 4. When the power-voltage derivative is positive($\frac{dP_{PV}}{dV_{PV}} > 0$), the PV array's output voltage (V_{PV}) rises, and when the voltage-management result is negative($\frac{dP_{PV}}{dV_{PV}} < 0$) as in (5)it falls[21].

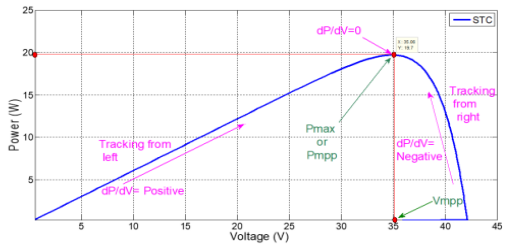

Fig.4The basic principle of MPPT for technical P&O

$$V_{MPP} = K_1 \int \frac{dP_{PV}}{dV_{PV}} dt \quad (5)$$

Because of its ease of use, low computing power requirements, and simplicity, P&O is a popular MPPT algorithm. By comparing the signs of the initial perturbation with the most recent spike in power, the next perturbation is calculated using the P&O MPPT approach. As part of this process, the operating voltage of the DC connection between the PV array and the DC/DC converter must be changed. Consequently, it must maintain a constant perturbation direction as power rises while changing it if power decreases. The technical was modelled using Matlab.

C. *Boost Converter*

The DC/DC boost converter is utilized to increase the output voltage of the PV array to the appropriate level. The DC/DC boost converter's switches and components are a diode, a MOSFET, and a capacitor and inductor[22]. The boost converter's storage components serve as a low-pass filter. When the converter input current varies due to switching, an input capacitor (C_a) stabilizes the PV array's terminal voltage, and an output capacitor (C_1)) acts as a low-pass filter to minimize the output voltage ripple. The operating modes of the DC/DC boost converter are displayed. Current flows clockwise between the inductor and the switch (Q) when the switch is actuated, storing energy in a magnetic field ($V_{La} = V_{Pv}$) [23]. The induced voltage across the inductor is polarised in the opposite direction when the switch (Q) is switched off, erasing the magnetic field formed to maintain the current flowing toward the DC connection. The output voltage (V_{dc}) will be larger than the input voltage ($V_{dc} = V_{Pv} + V_{La}$) because the inductor voltage (V_{La}) is added to the array voltage (V_{Pv}). MPPT is also used on the boost converter to optimize the power of the PV array when the sun's irradiance varies [24].

Consequently, the boost converter's switching duty cycle (D_y) is created. The capacity To act as a voltage source for boost converters is computed and connected to the PV array's output terminal. The input and output variables of the DC/DC boost converter, as well as the values of its components, may be calculated using the following (6) to (10) formulas:

$$C_a = \frac{D_y * V_{PV}}{4 * \Delta V_{PV} * {f_s}^2 * I_{dc}} \quad (6)$$

$$D_y = 1 - \frac{V_{PV}}{V_{dc}} \quad (7)$$

$$L_a = \frac{V_{PV} * (V_{dc} - V_{PV})}{\Delta I_{La} * f_s * V_{dc}} \quad (8)$$

$$\Delta I_{La} = 0.13 * I_{PV} * \frac{V_{dc}}{V_{PV}} \quad (9)$$

$$C_a \geq \frac{P_{PV}}{\Delta V_O * f_s * V_{dc}} \quad (10)$$

Where

V_{PV} input voltage to the converter from the PV array (V)

I_{PV} max current PV array (A)

P_{PV} Power PV (w)

f_s switching frequency (Hz)

C_a link capacitance PV array (F)

C_I DC link capacitance (F)

l_a Inductor boost (H)

V_{dc} output voltage boost (V)

D_y Duty cycle (boost converter)

ΔV_{PV} voltage change in PV (V)

ΔI_{La} current ripple of boost inductor (I)

ΔV_O Output voltage ripple (v).

D. *Buck Converter*

The buck is made up of a voltage source E, a capacitor C, a coil and a resistor R as a load, a diode D, and a switch Q; to satisfy the needed load, the coil's value was calculated using (11), and the capacitor's value was calculated using (12) [25].

$$L_{min} = \frac{(V_g - V_o)D}{\Delta i_L f} \quad (11)$$

$$C_{min} = \frac{(1 - D)V_o}{8Lf^2 \Delta i V_O} \quad (12)$$

E. *Alkaline Electrolyzer*

Alkaline Electrolyzer Modeled in Math electric energy, alkaline water electrolysis separates water into hydrogen and oxygen as in (13)to(15)show the chemical processes (3). Electrons convert water molecules to hydrogen and negatively charged hydroxide ions at the cathode, and Hydroxide is used as an anode. While releasing electrons, ions are oxidized to produce oxygen and water. A water molecule responds to a variety of things.

The proportions of hydrogen and oxygen are 2:1.

$$Cathod: \quad 2H_2O(l) + 2e^- \rightarrow H_2(g) + 2OH^-(\text{aq}) \quad (13)$$

$$Anode: \quad 2OH^- \rightarrow \frac{1}{2}O_2(g) + H_2O(l) + 2e^- \quad (14)$$

$$\text{Overall reaction: } H_2O(l) + 2e^- \rightarrow H_2(g) + \frac{1}{2}O_2(g) \quad (15)$$

An alkaline electrolyzer's performance is often evaluated by plotting its polarization curve(I-V) characteristic curve, which is obtained by comparing the cell voltage against the current density of the electrodes. The polarization curve of a typical alkaline electrolyzer considers some critical sources of cell voltage (V_{cell}) above the reversible potential (V_{rev}). As a result, the cell voltage will be higher than the reversible voltage of the same cell. Irreversible processes are to blame for this. For example, cell efficiency is reduced by overvoltage, which is irreversible [26]. The following are the primary sources:

- Electrolyte loss in the Ohmic range

- Oxygen causes an overvoltage.
- With hydrogen, there is an increase in voltage.
- Ohmic loss is caused by an ohmic loss in electrodes and circuits.

The voltage in an electrolysis cell can be defined as the sum of the reversible voltage and any additional overvoltage. In (16), it is defined as such. Reversible cell voltage (V_{rev}), activation overvoltage(V_{act}), ohmic loss overvoltage (V_{ohm}), and concentrations overvoltage (V_{con}) are all examples of overvoltage in this context. For electrolysis to occur, the reversible cell voltage must be at least the minimal value. The Gibbs equation can be used in (17) [27] to determine this.

Reversible voltage can be found by rearranging the Gibbs in (18) as follows.

$$V_{cell} = V_{rev} + V_{act} + V_{ohm} + V_{con} \tag{16}$$

$$\Delta G = zF\, V_{rev} \tag{17}$$

Where z is the number of electrons, F is Faraday's constant, ΔG is the Gibbs energy.

$$V_{rev} = \frac{\Delta G}{zF} \tag{18}$$

The Gibbs energy for water splitting at typical conditions (25 C° and 1 bar) is 237.2 kJ mol^{-1} [28], and the Faraday constant is 96485 $C.mol^{-1}$. In addition, the z is equal to 2. Substituting these numbers into the equation above yields the result.

$$V_{rev} = \frac{237.0 * 10^3}{2 * 96485} = 1.299\ V$$

Activation by Overvoltage(V_{act}) The activation overvoltage is generated by the simultaneous half-reactions of the anode and cathode. It takes much energy to transport electrons between the electrodes and chemical species. The electrode materials ' catalytic characteristics determine whether the charge may transfer from the reactants to the electrodes or vice versa. The activation voltage(V_{act}), which is a high voltage across the electrode, is generated [28]. The expression in (19) can be used to define.

$$V_{act} = s\log(\frac{t1 + \frac{t2}{T} + t3}{A} * I + 1) \tag{19}$$

On the other hand, the overvoltage coefficient on an electrode is the sum of the overvoltage coefficients on all electrodes (t_1, t_2, t_3, and A). Table 1 contains all the constants' values and units. The phenomenon of the Ohmic Type Voltage (V_{ohm}) is a measure of the cell's ohmic losses. Electrodes, interconnections, and the separating diaphragm contribute to losing electrons in a cell [27, 29]. Shortening the distance between the anode and the cathode can reduce it. Aside from that, it is a function of how much current flows through the cella as in (20) by [28] can be used to determine this overvoltage.

$$V_{ohm} = \frac{r1 + r2T}{A} I \tag{20}$$

The parameters r_1 and r_2 are connected to the electrolyte's ohmic resistance [27, 28]. Table 1 contains all the constants' values and units. Overvoltage Mass transport processes like convection and diffusion create concentration overvoltage. On the other hand, alkaline electrolysis often has a lower A concentration overvoltage age is omitted in this modeling work, and equation (16) can be expressed as in (21)(22).

$$V_{cell} = V_{rev} + V_{act} + V_{ohm} \tag{21}$$

$$V_{cell} = \frac{\Delta G}{zF} + s\log(\frac{t1 + \frac{t2}{T} + t3}{A} * I + 1) + \frac{r1 + r2T}{A} I \tag{22}$$

Furthermore, the hydrogen flow rate is presented in (23),

$$M_{H2} = \left(\frac{\left(\frac{I}{A}\right)^2}{f_1 + \left(\frac{I}{A}\right)^2} * f_2\right) * \frac{v_{cf}}{zF} \tag{23}$$

The parameters r_1 and r_2 are connected to the electrolyte's ohmic resistance [28]. Table 1 lists all the constants' values and units. Identifying the s, r1, r2, t1, t2, and t3 parameters resulted from adjusting the empirical I-V curves to (22) employing nonlinear regression methods using the *lsqcurvefit* function Optimization styles.

TABLE 1 CONSTANT PARAMETER

Constant parameters	***Symbols***	***Value***	***Unit***
Rev. Voltage	Vrev	1.229	V
Area of Electrode	A	400	$C\ m^2$
Faraday's Constant	F	96485	$Cmol^{-1}$
Number of Electrons	z	2	
The coef. for O.V on Electrodes	s	0.921	V
The coeff. for O.V on Electrodes	t1	0.09	$A^{-1}m^2$
The coef. for O.V on Electrodes	t2	12.345	$A^{-1}m^2C°$
The coef. for O.V on Electrodes	t3	534.760	$A^{-1}m^2C°$
Parameter Related to Ohmic Resistance of Electrolyte	r1	8.494×10^{-4}	Ωm^2
Parameter Related to Ohmic Resistance of Electrolyte	r2	1.166×10^{-4}	Ωm^2C^{o-1}

F. Storage tank modeling

Model for hydrogen storage Tanks may be used to store compressed hydrogen gas or liquid hydrogen in one of the hydrogen storage systems. We can explain how the hydrogen is stored using the tank's system dynamics as in (24): [30]

$$P_b - P_{bi} = z \times \frac{NH_2RT_b}{MH_2V_b} \tag{24}$$

P_b The pressure of the tank (pascal) P_{bi} The initial pressure of the storage tank(pascal) R universal (rydberg)gas constant (J/Kmol K) T_b operation temp. (K) V_b The volume of the tank in (m^3), Z is the compressibility factor as a function of pressure, P is the pressure, V_m is the molar volume, and T is the temperature as in (25):

$$z = \frac{PV_m}{RT} \tag{255}$$

In this concept, the ratio of hydrogen flow into the tank is employed to estimate tank pressure directly. [31]. The hydrogen storage Simulink model, does not incorporate additional power requirements, such as pumps, valves, fans, or compression motors[32] [33].

III. Results and Discussion

The mathematical model was simulated using MATLAB Simulink to analyze the Electrolyzer's behavior at a different voltage, current, and temperature, as shown in Fig. 5. The solar panels were modeled with MPPT by applying the P& O Technique. This technique regulates the PV array's output voltage and current to extract the most power and enhance overall PV system efficiency during solar radiation changes. Simulating this technique is shown in Fig.6. The electrolyzer modeling by applying the mathematical model according to the equation (22), as shown in Fig. 7, and the Hydrogen production modeling by applying the mathematical model according to (23), as shown in Fig. 8. Modeling the hydrogen gas tank according to the (24), as shown in Fig. 9

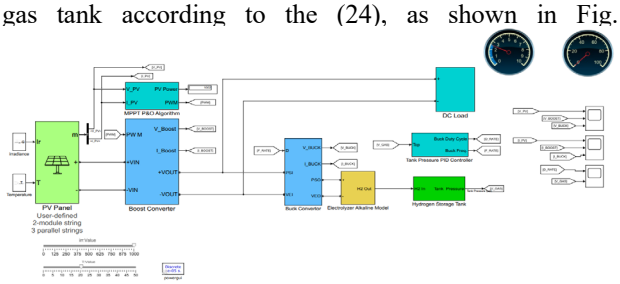

Fig. 5 Simulink model of energy storage system

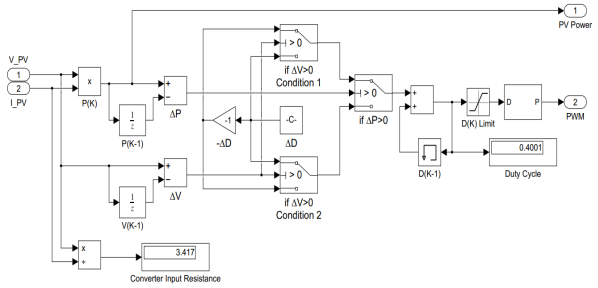

Fig.6 Simulink model of the P&O MPPT technique

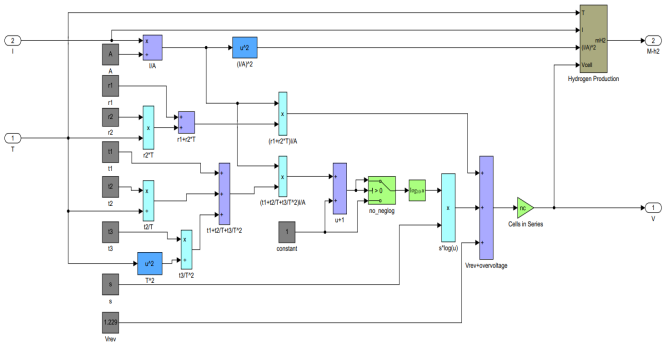

Fig. 7 Simulink model of Electrolyser

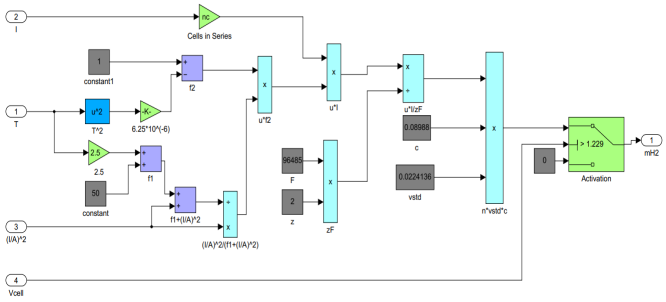

Fig. 8 Simulink model of Hydrogen production

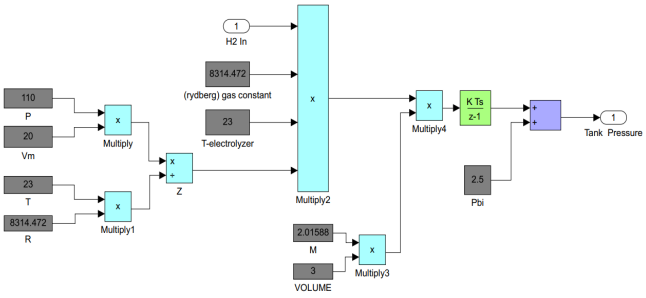

Fig. 9 Storage system hydrogen simulation

Furthermore, the gas tank was controlled by the fuzzy neural method. This controller combines two methods based on artificial intelligence techniques: artificial neural networks and fuzzy logic. Calculated hydrogen pressure safety is implemented using synthetic neural fuzzy heuristics systems. The data is entered into the Training of the ANFIS editor, as shown in Fig. 10. And then, the variable input rate of the MF editor interface is shown in Fig. 11. According to the results and systems, Training of fuzzy neural data as shown in Fig. 12 ANFIS is suitable for modeling more dynamic I/O and the rules followed as shown in Fig. 13 result. ANFIS was used to extinguish the electrolyte and stop the formation of hydrogen gas. Neuro-fuzzy's performance is better because it automatically determines the number of rules, reduces computational time, learns faster, and produces lower errors. It has been modeled, shown inFig. 14(a). The system shuts down when the tank pressure reaches the set level, As shown in Fig. 14(b).

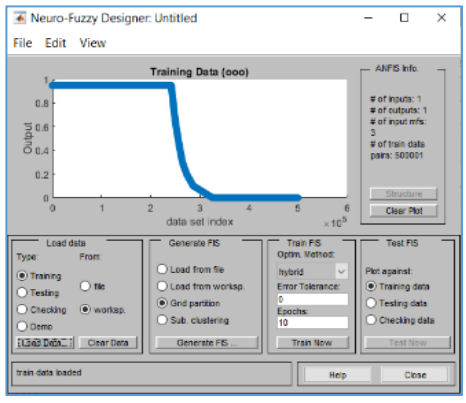

Fig. 10 Training data

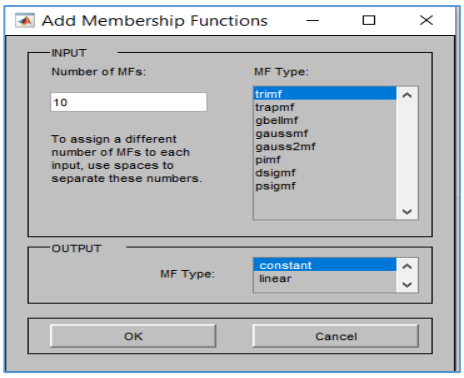

Fig. 11 Membership functions

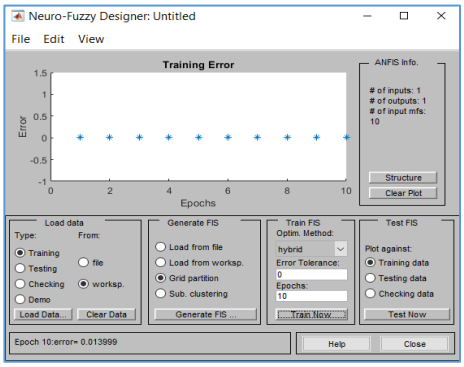

Fig. 12 Training Erorr

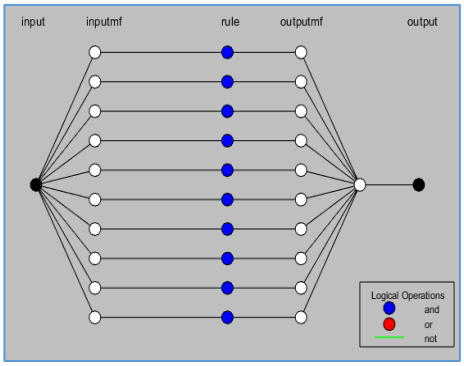

Fig. 13 Architecture of ANFIS model for the flow process

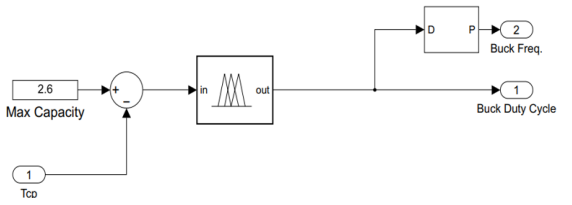

(a)

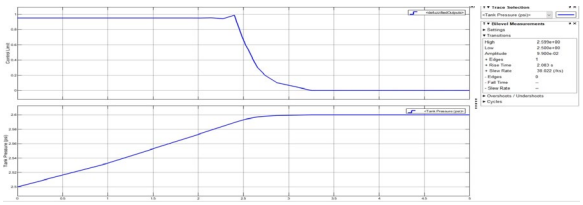

(b)

Fig. 14 Structure simulation and performance systema) Block of structure simulation of pressure ANFIS controller Model of fuzzy controller b) performance system

IV. Conclusion

This paper used MATLAB Simulink to simulate and evaluate the components of a solar energy storage system. Its main inputs are solar radiation and temperature, with hydrogen serving as a storage medium for solar energy. Hydrogen production allows for long-term storage of backup electrical energy used or injected into the low voltage grid. Hydrogen produced in cars can be used for transportation or in fuel cells to generate direct electrical power in a low-voltage grid. In this active system, each part was simulated using a model. The simulations revealed that the proposed hydrogen production cell type meets the engineering requirements. The HHO dry-cell temperature-based modeling approach is being expanded as part of this effort. Because of the explosive nature of Hydrogen gas, the tank pressure was controlled by a neuro-fuzzy method, so the hydrogen generation system was controlled and turned off when the specified tank pressure was reached.

References

[1] A. Andrijanovitš, M. Egorov, M. Lehtla, and D. Vinnikov, "New method for stabilization of wind power generation using an energy storage technology," *Journal on Agronomy Research,* vol. 8, no. S1, pp. 12-24, 2010.

[2] M. Faisal, M. A. Hannan, P. J. Ker, A. Hussain, M. B. Mansor, and F. Blaabjerg, "Review of energy storage system technologies in microgrid applications: Issues and challenges," *Ieee Access,* vol. 6, pp. 35143-35164, 2018.

[3] K. Nigim and H. Reiser, "Energy storage for renewable energy combined heat, power and hydrogen fuel (CHPH 2) infrastructure," in *2009 IEEE Electrical Power & Energy Conference (EPEC)*, 2009: IEEE, pp. 1-6.

[4] J. Moore and B. Shabani, "A critical study of stationary energy storage policies in Australia in an international context: the role of hydrogen and battery technologies," *Energies,* vol. 9, no. 9, p. 674, 2016.

[5] H. Shahinzadeh, S. Nikolovski, J. Moradi, and R. Bayindir, "A Resilience-Oriented Decision-Making Model for the Operation of Smart Microgrids Subject to Techno-Economic and Security Objectives," in *2021 9th International Conference on Smart Grid (icSmartGrid)*, 2021: IEEE, pp. 226-230.

[6] L. Bagherzadeh, H. Shahinzadeh, H. Shayeghi, and G. B. Gharehpetian, "A short-term energy management of microgrids considering renewable energy resources, micro-compressed air energy storage and DRPs," *International Journal of Renewable Energy Research (IJRER),* vol. 9, no. 4, pp. 1712-1723, 2019.

[7] H. Shahinzadeh, A. Gheiratmand, S. H. Fathi, and J. Moradi, "Optimal design and management of isolated hybrid renewable energy system (WT/PV/ORES)," in *2016 21st Conference on Electrical Power Distribution Networks Conference (EPDC)*, 2016: IEEE, pp. 208-215.

[8] B. Zakeri and S. Syri, "Electrical energy storage systems: A comparative life cycle cost analysis,"

Renewable sustainable energy reviews, vol. 42, pp. 569-596, 2015.

[9] F. Zhang, P. Zhao, M. Niu, and J. Maddy, "The survey of key technologies in hydrogen energy storage," *International journal of hydrogen energy,* vol. 41, no. 33, pp. 14535-14552, 2016.

[10] A. M. Abdalla, S. Hossain, O. B. Nisfindy, A. T. Azad, M. Dawood, and A. K. Azad, "Hydrogen production, storage, transportation and key challenges with applications: A review," *Energy conversion and management,* vol. 165, pp. 602-627, 2018.

[11] J. Li, W. Liu, and W. Qi, "Hydrogen production technology by electrolysis of water and its application in renewable energy consumption," in *E3S Web of Conferences*, 2021, vol. 236: EDP Sciences, p. 02001.

[12] M. David, C. Ocampo-Martínez, and R. Sánchez-Peña, "Advances in alkaline water electrolyzers: A review," *Journal of Energy Storage,* vol. 23, pp. 392-403, 2019.

[13] C. Varela, M. Mostafa, and E. Zondervan, "Modeling alkaline water electrolysis for power-to-x applications: A scheduling approach," *International journal of hydrogen energy,* vol. 46, no. 14, pp. 9303-9313, 2021.

[14] D. Jang, H.-S. Cho, and S. Kang, "Numerical modeling and analysis of the effect of pressure on the performance of an alkaline water electrolysis system," *Applied Energy,* vol. 287, p. 116554, 2021.

[15] M. Rizwan, "Dynamic modeling and control of a system of electrolyzers for hydrogen production," *Specialization project report, NTNU,* 2019.

[16] D. Martinez and R. Zamora, "MATLAB simscape model of an alkaline electrolyser and its simulation with a directly coupled PV module," *International Journal of Renewable Energy Research,* vol. 8, no. 1, pp. 552-560, 2018.

[17] F. A. Kareem, N. S. Lafta, and D. Z. Khalaf, "Energy and Exergy Analysis of the Solar Radiation Incident over Iraq," in *IOP Conference Series: Materials Science and Engineering*, 2019, vol. 518, no. 3: IOP Publishing, p. 032008.

[18] B. Aïssa, R. J. Isaifan, V. E. Madhavan, and A. A. Abdallah, "Structural and physical properties of the dust particles in Qatar and their influence on the PV panel performance," *Scientific reports,* vol. 6, no. 1, pp. 1-12, 2016.

[19] K. SUBBARAO and K. P. KALYAN, "Comparitive Analysis of a MPPT Control Techniques," 2021.

[20] A. F. Nematollahi, H. Shahinzadeh, H. Nafisi, B. Vahidi, Y. Amirat, and M. Benbouzid, "Sizing and Sitting of DERs in Active Distribution Networks Incorporating Load Prevailing Uncertainties Using Probabilistic Approaches," *Applied Sciences,* vol. 11, no. 9, p. 4156, 2021.

[21] M. J. Hasan, "Modeling and simulation of 1kw single phase grid tied inverter for solar photovoltaic system," in *IOP Conference Series: Materials Science and Engineering*, 2020, vol. 881, no. 1: IOP Publishing, p. 012139.

[22] M. J. Hasan and F. A. M. Al-Qrimli, "Single-Phase, H-Bridge 3-level Inverter of Wide Range Input Voltage for Grid Connected Solar Photovoltaic Applications," *International Journal of Computer Applications,* vol. 975, p. 8887.

[23] K. Jain, M. Gupta, and A. K. Bohre, "Implementation and comparative analysis of P&O and INC MPPT method for PV system," in *2018 8th IEEE India International Conference on Power Electronics (IICPE)*, 2018: IEEE, pp. 1-6.

[24] S. Singh, S. Manna, M. I. H. Mansoori, and A. Akella, "Implementation of Perturb & Observe MPPT Technique using Boost converter in PV System," in *2020 International Conference on Computational Intelligence for Smart Power System and Sustainable Energy (CISPSSE)*, 2020: IEEE, pp. 1-4.

[25] S. M. Ghamari, H. Mollaee, and F. Khavari, "Robust self-tuning regressive adaptive controller design for a DC–DC BUCK converter," *Measurement,* vol. 174, p. 109071, 2021.

[26] A. Ursúa and P. Sanchis, "Static–dynamic modelling of the electrical behaviour of a commercial advanced alkaline water electrolyser," *International journal of hydrogen energy,* vol. 37, no. 24, pp. 18598-18614, 2012.

[27] A. S. Tijani, N. A. B. Yusup, and A. A. Rahim, "Mathematical modelling and simulation analysis of advanced alkaline electrolyzer system for hydrogen production," *Procedia Technology,* vol. 15, pp. 798-806, 2014.

[28] Ø. Ulleberg, "Modeling of advanced alkaline electrolyzers: a system simulation approach," *International journal of hydrogen energy,* vol. 28, no. 1, pp. 21-33, 2003.

[29] K. Mazloomi, N. B. Sulaiman, and H. Moayedi, "Electrical efficiency of electrolytic hydrogen production," *International Journal of Electrochemical Science,* vol. 7, no. 4, pp. 3314-3326, 2012.

[30] E. M. Zakaria, S. H. Arafa, M. M. Nashed, and S. G. Ramadan, "Dynamic Analysis of Photovoltaic-Fuel Cell-Electrolyzer System at Stand Alone Operation," *nternational Journal of Engineering Innovative Technology Volume,* vol. 8, pp. 7-12.

[31] S. Nasri, S. B. Slama, I. Yahyaoui, B. Zafar, and A. Cherif, "Autonomous hybrid system and coordinated intelligent management approach in power system operation and control using hydrogen storage," *nternational journal of hydrogen energy,* vol. 42, no. 15, pp. 9511-9523, 2017.

[32] M. A. Al-Refai, "Matlab/Simulink Simulation of Solar Energy Storage System," *International Journal of Electrical and Computer Engineering,* vol. 8, no. 2, pp. 297-302, 2014.

[33] T. Lajnef, S. Abid, and A. Ammous, "Modeling, Control, and Simulation of a Solar Hydrogen/Fuel Cell Hybrid Energy System for Grid-Connected Applications," *Advances in Power Electronics,* 2013.